Journal of Neuro-Oncology (2020) 147:681–690
https://doi.org/10.1007/s11060-020-03475-y

CLINICAL STUDY

Differentiation of progressive disease from pseudoprogression using 3D PCASL and DSC perfusion MRI in patients with glioblastoma

Paul Manning[1,2,6] · Shadi Daghighi[1,2] · Matthew K. Rajaratnam[2] · Sowmya Parthiban[2] · Naeim Bahrami[2] · Anders M. Dale[1,2,3] · Divya Bolar[1,4] · David E. Piccioni[3] · Carrie R. McDonald[2,3,5] · Nikdokht Farid[1,2]

Received: 26 December 2019 / Accepted: 24 March 2020 / Published online: 1 April 2020

Abstract

Purpose To use 3D pseudocontinuous arterial spin labeling (3D PCASL) and dynamic susceptibility contrast-enhanced (DSC) perfusion MRI to differentiate progressive disease from pseudoprogression in patients with glioblastoma (GBM).

Methods Thirty-two patients with GBM who developed progressively enhancing lesions within the radiation field following resection and chemoradiation were included in this retrospective, single-institution study. The updated modified RANO criteria were used to establish progressive disease or pseudoprogression. Following 3D PCASL and DSC MR imaging, perfusion parameter estimates of cerebral blood flow (ASL-nCBF and DSC-nrCBF) and cerebral blood volume (DSC-nrCBV) were calculated. Additionally, contrast enhanced volumes were measured. Mann–Whitney U tests were used to compare groups. Linear discriminant analysis (LDA) and area under receiver operator characteristic curve (AUC) analyses were used to evaluate performance of each perfusion parameter and to determine optimal cut-off points.

Results All perfusion parameter measurements were higher in patients with progressive disease (mean, 95% CI ASL-nCBF 2.48, [2.03, 2.93]; DSC-nrCBF = 2.27, [1.85, 2.69]; DSC-nrCBV = 3.51, [2.37, 4.66]) compared to pseudoprogression (mean, 95% CI ASL-nCBF 0.99, [0.47, 1.52]; DSC-nrCBF = 1.05, [0.36, 1.74]; DSC-nCBV = 1.19, [0.34, 2.05]), and findings were significant at the $p < 0.0125$ level ($p = 0.001$, 0.003, 0.002; effect size: Cohen's $d = 1.48$, 1.27, and 0.92). Contrast enhanced volumes were not significantly different between groups ($p > 0.447$). All perfusion parameters demonstrated high AUC (0.954 for ASL-nCBF, 0.867 for DSC-nrCBF, and 0.891 for DSC-nrCBV), however, ASL-nCBF demonstrated the highest AUC and misclassified the fewest cases (N = 6). Lesions correctly classified by ASL but misclassified by DSC were located along the skull base or adjacent to large resection cavities with residual blood products, at areas of increased susceptibility.

Conclusion Both 3D PCASL and DSC perfusion MRI techniques have nearly equivalent performance for the differentiation of progressive disease from pseudoprogression in patients with GBM. However, 3D PCASL is less sensitive to susceptibility artifact and may allow for improved classification in select cases.

Keywords ASL · DSC · Pseudoprogression · GBM · mRANO

✉ Paul Manning
pmanning@ucsd.edu

[1] Department of Radiology, University of California, San Diego, La Jolla, CA 92037, USA

[2] Center for Multimodal Imaging and Genetics, University of California, San Diego, La Jolla, CA 92037, USA

[3] Department of Neurosciences, University of California, San Diego, La Jolla, CA 92037, USA

[4] Center for Functional Magnetic Resonance Imaging, University of California, San Diego, La Jolla, CA 92037, USA

[5] Department of Psychiatry, University of California, San Diego, La Jolla, CA 92037, USA

[6] Department of Radiology, University of California, San Diego, 200 West Arbor Drive, Mailbox # 8756, San Diego, CA 92103, USA

Introduction

Glioblastoma (GBM) is the most common primary malignant brain tumor in the United States accounting for approximately 46% of all primary malignant brain tumors [1]. Prognosis for patients with GBM is poor with estimated 5-year survival rates ranging from 1.9 to 9.8% [1, 2]. Standard first-line treatment includes maximum feasible resection followed by a combination of radiotherapy and chemotherapy (temozolomide) [2, 3]. An ongoing challenge in the treatment of GBM is evaluation of treatment response. To address this, the Response Assessment in Neuro-Oncology (RANO) criteria was developed to provide a standardized framework to guide treatment response assessment in high-grade gliomas [4]. Ideally, treatment response could be assessed non-invasively using imaging, thereby avoiding morbidity related to biopsy or re-resection. However, current conventional MRI techniques are insufficient and can be confounded by post-treatment change and the phenomenon of "pseudoprogression". Per the RANO criteria, pseudoprogression is radiologically defined as new or enlarging area(s) of contrast enhancement occurring early after the completion of radiotherapy in the absence of true tumor growth, which subsides or stabilizes without a change in therapy [4, 5]. Although the mechanism of pseudoprogression is incompletely understood, it is thought to be due to radiation effects, likely potentiated by temozolomide, resulting in transient blood–brain barrier breakdown leading to increased edema and contrast enhancement.

Recently, an updated version of the RANO criteria has been developed, the modified RANO (mRANO), which further refines criteria for the evaluation of treated GBMs and provides additional guidance with regards to post-treatment change and pseudoprogression [6]. The new mRANO criteria recommend using the post-radiation scan as the reference or baseline scan to avoid the transient unpredictable (and potentially confounding) radiologic changes that occur between the post-surgical scan and post-radiation scan. Additionally, the mRANO criteria now provides clear radiologic response rubrics for the assessment of pseudoprogression, thus clarifying some previous areas of ambiguity and allowing for an improved systematic approach to treatment response assessment. However, even with the updated criteria, conventional MRI remains the primary modality for evaluation, and differentiation of progressive disease from pseudoprogression is assessed retrospectively based on follow-up exams [6]. For these reasons, there is active investigation into advanced imaging techniques to conclusively differentiate progressive disease from pseudoprogression, which would aid important treatment decisions such as clinical trial eligibility and whether to continue or change therapy [7].

Perfusion-weighted MR imaging techniques have shown promise in this regard, especially dynamic susceptibility contrast (DSC) perfusion MRI. DSC-MRI allows for estimation of tissue microvascular density through the measurement of cerebral blood volume (CBV) or cerebral blood flow (CBF) [8, 9]. High-grade gliomas like GBM exhibit marked microvascular proliferation and prominent angiogenesis [10–12], whereas areas of pseudoprogression or radiation necrosis are characterized by small vessel injury and ischemia [13]. By exploiting these differences, DSC-derived measurements of CBV and CBF have been shown to accurately differentiate recurrent GBM from radiation necrosis and predict overall survival [14–16]. There are, however, limitations associated with DSC-MRI. DSC-MRI is reliant on gadolinium based contrast agents (GBCAs), some of which have been associated with nephrogenic systemic fibrosis in patients with poor renal function [17] and all of which are deposited throughout the body and neuronal tissue regardless of renal function [18]. A well-known issue with DSC-MRI is that during imaging the contrast bolus may "leak" into the extravascular space at areas of blood–brain barrier disruption (typical for areas of enhancing tumor) and the resultant T1-relaxation effects can cause underestimation of the true CBV. Although several correction algorithms have been developed, each has pros and cons and there is no consensus agreement [19–21]. Furthermore, variability in processing techniques result in heterogeneous cut-off values that may not be comparable between studies [20, 22]. Finally, DSC-MRI is most often performed as a gradient-echo sequence where susceptibility artifact can preclude lesion evaluation, especially along the skull base, paranasal sinuses, and adjacent to areas of hemorrhage, including along resection cavity margins [20].

Arterial spin labeling (ASL) is an alternative non-contrast perfusion-weighted MR imaging technique which continues to gain traction and may offer some advantages over GBCA-based forms of perfusion MR imaging. ASL uses arterial blood flow as an endogenous tracer by magnetically labeling inflowing arterial blood through the use of radiofrequency (RF) inversion pulses, ultimately allowing for absolute tissue perfusion measurements [23, 24]. With the advent of newer ASL techniques, particularly the current white paper-recommended three-dimensional pseudocontinuous ASL (3D PCASL) sequence [25], ASL has become an increasingly popular choice for perfusion imaging. ASL has shown promise in neuro-oncologic applications including the evaluation of brain tumor perfusion [26–28] and differentiation of low-grade from high-grade glioma [29, 30]. Several studies have evaluated ASL for the differentiation of recurrent tumor from treatment effects, with early studies indicating that ASL may be an alternative perfusion MR imaging technique for this purpose [31–36]. However, the majority of these studies were performed in mixed patient

cohorts with both low- and high-grade gliomas [31–34] where differences in treatment regimens [37], enhancement patterns [38], and perfusion characteristics [26, 29, 30] make results less generalizable to patients with GBM. Additionally, previous studies have used variable imaging criteria to define progressive disease and treatment effects, not always based on an established framework like the RANO or mRANO criteria. Finally, several studies were performed using older less optimized versions of ASL [31, 35, 36], sometimes using mixed qualitative and semi-quantitative analysis methods [36].

The purpose of this study is to extend the literature evaluating the utility of 3D PCASL compared to DSC-MRI in several ways. First, we test the ability of ASL versus DSC-MRI to differentiate progressive disease from pseudoprogression. Importantly, we define pseudoprogression using the updated mRANO criteria, using the post-radiation scan as the baseline scan, thereby reducing the confounding radiologic changes following surgery. In addition, we limit our study to a well-characterized cohort of patients with GBM treated with standard of care chemoradiation. Based on the extant literature, we hypothesized that both ASL and DSC perfusion MR imaging techniques would differentiate progressive disease from pseudoprogression with high accuracy, however, we suspect that ASL may offer some advantages over DSC-MRI because it is not reliant on contrast injection, is less affected by susceptibility artifact, and allows for absolute perfusion measurements.

Materials and methods

Study design and patients

This retrospective, observational, single-institution study was approved by an Institutional Review Board and was compliant with the Health Insurance Portability and Accountability Act. Between May 2015 and November 2018, 139 adults with GBM were identified who underwent clinical MR evaluation which included 3D PCASL and DSC-MRI sequences. From this group, 32 patients were selected who met the following inclusion criteria: (i) confirmed diagnosis of GBM following gross or subtotal resection, (ii) received standard of care radiotherapy and chemotherapy (temozolomide), (iii) baseline post-radiation contrast-enhanced MRI was performed, (iv) subsequently developed an enlarging enhancing lesion within the radiation field measuring at least 10 mm in two perpendicular dimensions on axial images, (v) the enhancing lesion was detected on an MRI scan which included both 3D PCASL and DSC sequences, (vi) a final diagnosis of progressive disease or pseudoprogression was made based on histologic evaluation (when available) or combined radiologic and clinical evaluation using the mRANO criteria with final consensus decision made by a neuroradiologist and neurooncologist, both blinded to perfusion MR data, incorporating clinical information including clinical status (symptomatic deterioration) and recent steroid administration. For this study, radiologic pseudoprogression was defined as a new or increased measurable enhancing lesion, that was stable or resolving on serial MRIs over a minimum time period of 6 months, without a change in therapy.

MR exams

All MR exams were performed on a 3T MRI scanner (Discovery 750, GE Healthcare, Milwaukee Wisconsin) using an 8-channel brain array coil. Conventional MRI protocol included post-contrast 3D T1-weighted fast spoiled gradient-echo (FSPGR) imaging (TE/TR = 3.0/6.9 ms; FA = 9°; FOV = 25 cm; matrix = 256 × 256). Contrast enhanced exams were performed using either gadobenate dimeglumine (Bracco Diagnostics) or gadobutrol (Bayer AG) both at 0.1 mmol/kg.

ASL perfusion MRI was performed using pseudo-continuous (PCASL) labeling with a 3D stack-of-spirals fast spin echo readout; this reflects the GE product ASL sequence. PCASL-specific parameters included a labeling duration of 1450 ms and post labeling delay of 2025 ms with 3D spiral readout parameters as follows: spiral interleaves = 8; points per spiral = 512; slices = 36; slice thickness 4.0–4.2 mm; FOV = 24–26 cm; in-plane resolution = 3.64–4.53 mm^2; bandwidth = 62.5 kHz; TE = 9.5–10.5 ms; TR = 4800–4847 ms; NEX = 3; and scan time = 4 min 32 s–4 min 42 s.

DSC perfusion MRI was performed using a gradient-echo echo-planar-imaging (EPI) sequence (TE/TR = 35/1600 ms; FA = 90°; slice thickness 5 mm with intersection gap of 1 mm; 22 axial slices; FOV = 25 cm; matrix = 96 × 96) 0.1 mmol/kg of gadobenate dimeglumine (Bracco Diagnostics) or gadobutrol (Bayer AG), was injected intravenously with an MR-compatible power injector at a rate of 2–3 mL/s through an antecubital angiocatheter, followed immediately by a 20-mL continuous saline flush. The multi-section image set was acquired every 1–2 s during the first pass of the contrast agent until 60 time points were obtained [39]. Because no post-processing leakage correction was applied, a preload bolus was performed prior to image acquisition (1/4 dose, 0.025 mmol/kg) to balance the expected T1-weighting related to contrast leakage. In a small subset of patients (8/32) an alternate DSC-MRI acquisition method was used to balance competing T1 and T2* effects related to contrast leakage, using a low flip angle (FA = 25°) without preload bolus.

Image analysis

Maps of ASL-derived CBF were generated from the 3D PCASL images using ReadyView ASL (GE Healthcare), and maps of DSC-derived rCBF and rCBV were generated from the DSC-MRI images using ReadyView BrainStat AIF (GE Healthcare).

The ASL-CBF, DSC-rCBF, and DSC-rCBV maps were fused with post-contrast T1-weighted images using Volume Viewer (GE Healthcare) with single fusion mode, generating fused perfusion and contrast-enhanced images. Using the fused images, a board certified neuroradiologist with 10 years of experience and an image analyst with 2 years of experience who were blinded to patient clinical and pathologic data placed separate circular ROIs on each perfusion map corresponding to the regions of enhancement with greatest perfusion signal. Areas of necrosis, surgical cavities, vessels, hemorrhage, and susceptibility artifact were avoided. An additional ROI was placed on the contralateral "normal-appearing" brain at a corresponding anatomic location. Normalized values for each perfusion parameter (ASL-nCBF, DSC-nrCBF, and DSC-nrCBV) were calculated by dividing the mean signal intensity within the ROI at the region of enhancement by the mean signal intensity within the contralateral ROI.

Contrast-enhancement volumes (CE_{vol}) were measured by manually drawing volumes of interest on the post-contrast 3D FSPGR images, excluding areas of necrosis and surgical cavities, using semi-automatic segmentation methods (Amira software package, Visage Imaging). All volumes of interest (VOIs) were drawn by three trained image analysts and approved by the board-certified neuroradiologist.

Statistical analysis

Statistical analyses were performed using IBM SPSS, Version 26 (Armonk, New York). Group differences (progressive disease vs pseudoprogression) for each perfusion parameter (ASL-nCBF, DSC-nrCBF, and DSC-nrCBV) and for CE_{vol} were evaluated using Mann–Whitney U tests. To account for multiple comparisons, we applied Bonferroni correction and set our p-value to 0.05/4 = 0.0125. Stepwise linear discriminant analysis (LDA) using leave-one-out cross validation was performed to determine the set of parameters (ASL-nCBF, DSC-nrCBF, and DSC-nrCBV) that best classified patients as progressive disease vs pseudoprogression. LDA was favored for analysis because LDA can provide a robust classification model in situations of small sample sizes, given underlying assumptions are satisfied, including normally distributed predictive variables with equal variance/covariance [40]. Receiver operating characteristic (ROC) curves were generated and optimal cut-off values were determined for each perfusion parameter. Area under the ROC curve (AUC) was used to evaluate classifier performance. Unlike DSC-MRI, ASL allows for the evaluation of absolute CBF; therefore, separate analyses were performed to evaluate performance of absolute ASL-CBF.

Results

Patient population

Thirty-two adults with GBM (22 male) met inclusion criteria with ages ranging from 19 to 75 years (mean 56 ± 13 years). Progressive disease was diagnosed in 25 patients and pseudoprogression in 7 patients. Pathology was available for 9 patients (8 for progressive disease and 1 for pseudoprogression), and clinicoradiologic assessment was used to establish diagnosis in the remaining 23 patients (17 progressive disease and 6 pseudoprogression). Median time between post-radiation scan and pathologic or clinicoradiologic assessment was 5 months. Descriptive information on the patient cohort is provided in Table 1.

Quantitative perfusion parameter analysis

Inter-reader agreement was excellent for all three perfusion parameters with intraclass correlation coefficient's measuring 0.937 for ASL-nCBF, 0.908 for DSC-nrCBF, and 0.982 for DSC-nrCBV.

For all three perfusion parameters, measurements were higher in the progressive disease group (mean, 95% CI ASL-nCBF = 2.48, [2.03, 2.93]; DSC-nrCBF = 2.27, [1.85, 2.69]; DSC-nrCBV = 3.51, [2.37, 4.66]) compared to the pseudoprogression group (mean, 95% CI ASL-nrCBF = 0.99, [0.47, 1.52]; DSC-nrCBF = 1.05, [0.36, 1.74]; DSC-nCBV = 1.19, [0.34, 2.05]) and findings were significant at the $p < 0.01$ level (ASL-nCBF: U = 167, p = 0.001; DSC-nrCBF: U = 152, p = 0.003; DSC-nrCBV: U = 156, p = 0.002) (Fig. 1). Effect size estimates were large for all three perfusion parameters (Cohen's d = 1.48, 1.27, and 0.92) but were largest for ASL-nCBF. Measurements of CE volume were not significantly different between progressive disease and pseudoprogression groups (U = 105; p = 0.447).

Stepwise LDA including all three perfusion parameters demonstrated that ASL-nCBF was the strongest predictor and the only one retained in the model, correctly classifying 81.3% of the original and cross-validated sample ($\chi^2 = 9.87$; p = 0.002).

AUCs for each parameter were as follows: ASL-nCBF = 0.954, DSC-nrCBF = 0.867, and DSC-nrCBV = 0.891 (Fig. 2). Optimal cut-off values for classification were calculated for each perfusion parameter and ASL-nCBF demonstrated the highest sensitivity and specificity for classification. For ASL-nCBF a cut-off value of

Table 1 Descriptive characteristics of patient cohort

Patient number	Age	Sex	Resection	Time between radiotherapy and PD vs PSP (months)	Pathology available	Final diagnosis
1	69	F	GTR	2	No	PD
2	41	M	STR	4	No	PSP
3	60	M	STR	3	No	PSP
4	56	M	GTR	40	Yes	PD
5	59	M	STR	26	No	PD
6	68	M	GTR	31	No	PD
7	53	F	STR	20	No	PD
8	44	M	GTR	2	No	PD
9	58	M	STR	13	Yes	PD
10	50	M	STR	9	Yes	PSP
11	75	M	STR	2	No	PD
12	61	F	GTR	6	No	PSP
13	19	M	STR	11	No	PD
14	45	M	STR	3	No	PSP
15	61	F	GTR	9	Yes	PD
16	61	M	GTR	4	No	PD
17	62	M	GTR	2	No	PD
18	65	M	STR	10	No	PD
19	57	M	STR	3	No	PD
20	20	M	GTR	6	Yes	PD
21	52	F	STR	20	No	PD
22	74	M	STR	4	No	PD
23	55	M	STR	1	No	PSP
24	56	F	STR	7	Yes	PD
25	68	F	STR	7	No	PD
26	60	F	STR	28	No	PD
27	59	F	STR	3	No	PD
28	54	M	STR	4	No	PD
29	60	M	GTR	3	No	PD
30	58	F	STR	9	Yes	PD
31	53	M	GTR	3	No	PD
32	63	M	GTR	4	Yes	PSP

M male, *F* female, *GTR* gross total resection, *STR* Subtotal resection, *PD* progressive disease, *PSP* pseudoprogression

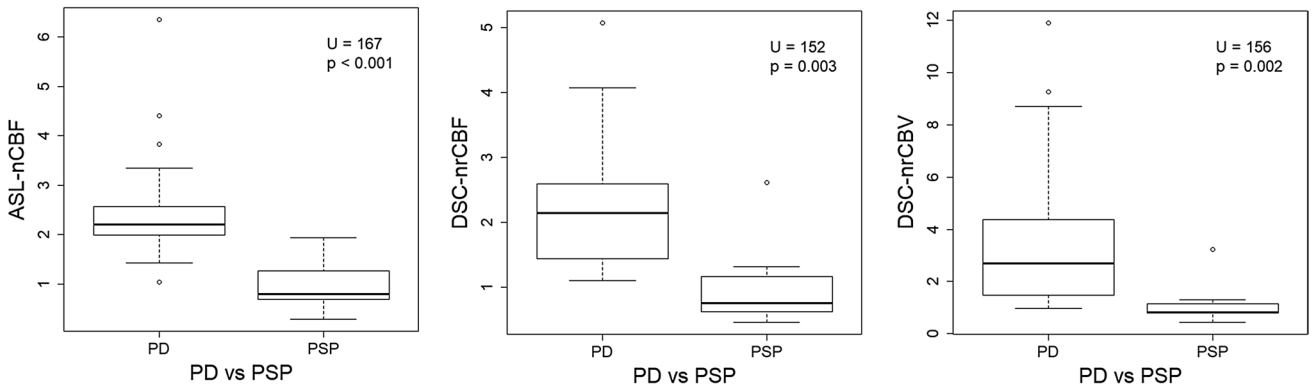

Fig. 1 Boxplots demonstrating perfusion parameter values (ASL-nCBF, DSC-nCBF, and DSC-nCBV) for progressive disease compared to pseudoprogression. The median value; 1st, 2nd, 3rd, and 4th quartiles; and the minimum and maximum values of each perfusion parameter are indicated. Plots are annotated with the U-statistic and the p-value from the Mann–Whitney U test for each comparison

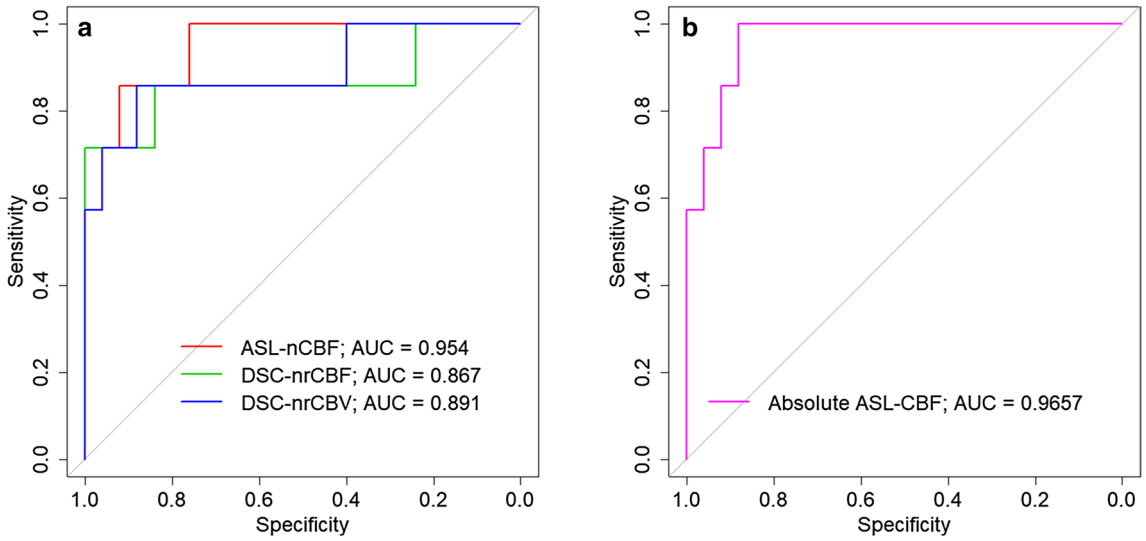

Fig. 2 Receiver operator characteristic (ROC) curves for differentiating progressive disease from pseudoprogression by each perfusion parameter (ASL-nCBF, DSC-nCBF, and DSC-nCBV) with corresponding area under the ROC curve (AUC) displayed (**a**). ROC curve for differentiating progressive disease from pseudoprogression by absolute ASL-CBF with corresponding AUC displayed (**b**)

1.570 yielded a sensitivity of 0.920 and specificity of 0.857, for DSC-nrCBF a cut-off value of 1.335 yielded a sensitivity of 0.840 and specificity of 0.857, and for DSC-nrCBV a cut-off value of 1.335 yielded a sensitivity of 0.880 and specificity of 0.857 (Fig. 2a).

Based on the optimal cut-off values, ASL-nCBF misclassified the fewest cases. In total, 6 cases were misclassified by ASL-nCBF, 10 by DSC-nrCBF, and thirteen by DSC-nrCBV. Analysis of the six cases which were correctly classified by ASL-nCBF but misclassified by both DSC-nrCBF and DSC-nrCBV revealed that all six of these lesions were located along the skull base, adjacent to the paranasal sinuses, or adjacent to a large resection cavity with residual blood products where prominent susceptibility artifact obscured the lesion (Figs. 3, 4). Analysis of the two cases which were misclassified by ASL-nCBF but correctly classified by DSC-nrCBF or DSC-nrCBV did not demonstrate the same relationship to susceptibility artifact. However, in these two cases the measurements were relatively close to the cut-off values. The discrepancies could have been related to mixed lesions (overlapping areas of progression and pseudoprogression) or possibly imprecise measurement using ROI methods rather than histogram methods, although these justifications are speculative.

Absolute ASL-CBF measurements were also significantly higher in the progressive disease group compared to the pseudoprogression group ($U = 169$, $p < 0.001$). AUC evaluation similarly showed high performance for ASL-CBF, measuring 0.966, with a cut-off value of 64.2 mL/100 g/min yielding sensitivity of 1.000 and specificity of 0.880 (Fig. 2b).

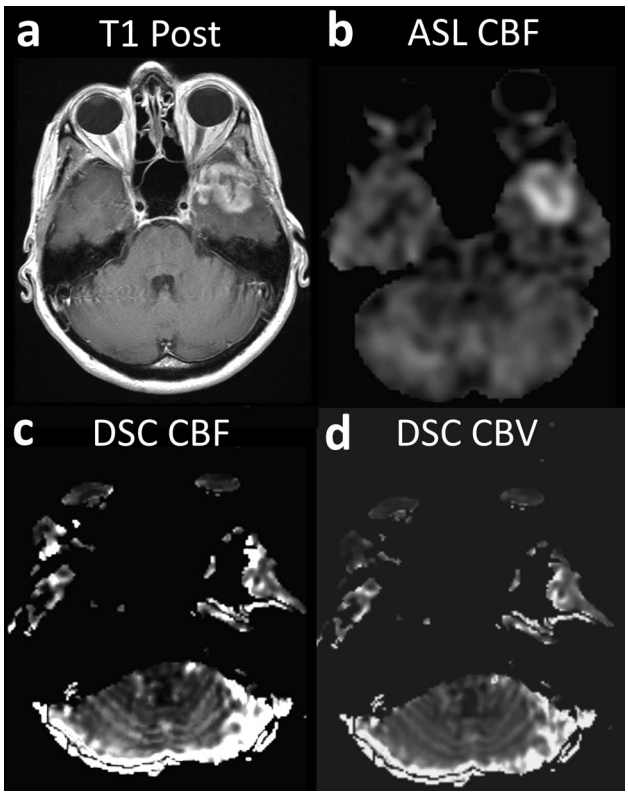

Fig. 3 Example case demonstrating a lesion located along the skull base with T1 post-contrast (**a**), ASL-nCBF (**b**), DSC-nCBF (**c**), and DSC-nCBV (**d**) images included. This case was correctly classified as progressive disease by ASL-nCBF, but incorrectly classified by both DSC-nCBF and DSC-nCBV. Prominent susceptibility artifact from the adjacent paranasal sinuses obscures lesion evaluation on DSC-MR images

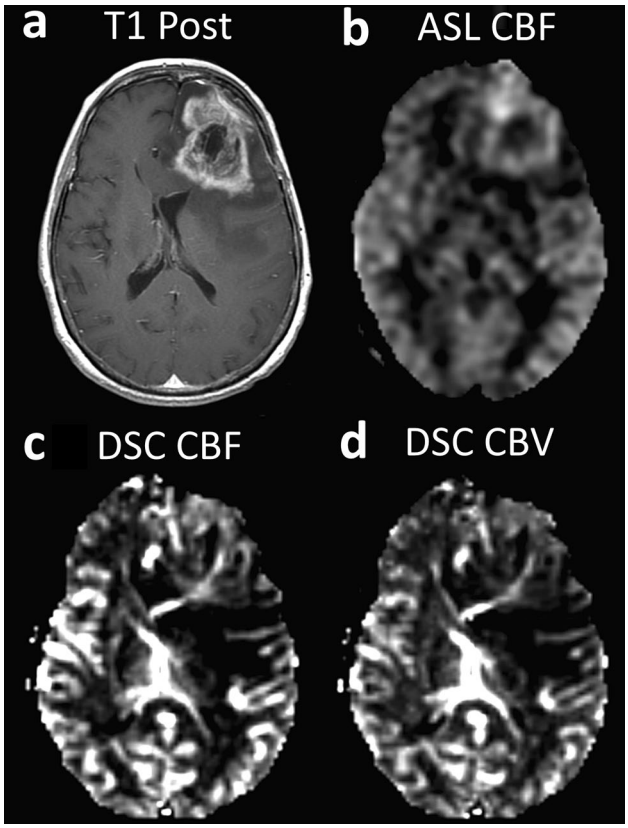

Fig. 4 Example case demonstrating a lesion located adjacent to a large resection cavity with T1 post-contrast (**a**), ASL-nCBF (**b**), DSC-nCBF (**c**), and DSC-nCBV (**d**) images included. This case was correctly classified as progressive disease by ASL-nCBF, but incorrectly classified by both DSC-nCBF and DSC-nCBV. In this example, susceptibility artifact related to the resection cavity and blood products obscures lesion evaluation on DSC-MR images

Discussion

We evaluated the utility of 3D PCASL compared to DSC-MRI for the differentiation of progressive disease from pseudoprogression in patients with treated GBM, as defined by the combination of the updated mRANO criteria and our requirement for at least 6 months without a change in treatment to qualify as pseudoprogression. We demonstrate that both 3D PCASL and DSC perfusion MRI techniques can be used for differentiation with high accuracy and nearly equivalent performance. However, there are select cases where 3D PCASL provides improved evaluation, especially in areas strongly affected by susceptibility artifact.

Our results are in concordance with several recent studies revealing that both ASL and DSC perfusion MRI techniques can be used for differentiation of recurrent glioma from treatment effects with nearly equivalent performance [31–36]. Compared to two recent studies [32, 33], we report higher performance for all perfusion parameters. This may be because prior studies were performed in mixed cohorts that included patients with both low- and high-grade gliomas [31–34]. In comparison to high-grade gliomas, low-grade gliomas have a different incidence of pseudoprogression [41], different treatment algorithms [37], different conventional contrast-enhanced MR findings [38], and much lower baseline DSC- and ASL-derived perfusion measurements [26, 29, 30]. For these reasons, radiologic treatment response (including perfusion imaging) is expected to be quite different in low-grade gliomas, making conclusions drawn from mixed cohorts less generalizable to patients with GBM.

A strength of our study is the use of newer and more conservative definitions to define progressive disease and pseudoprogression compared to prior studies. Although histology is generally considered the gold standard in determination of progressive disease and pseudoprogression, even histology can be complicated by tissue sampling error, mixed lesions, and inter-observer differences [42]. For these reasons radiologic evaluation continues to play an important role, however, radiologic evaluation can be hindered by heterogeneity in methods and ambiguity in terminology. To address these issues, we use the updated mRANO criteria to provide a standard framework for evaluation of radiologic treatment response. The mRANO criteria builds upon the prior RANO criteria by improving the reference or baseline scan to the post-radiation scan, thereby avoiding the transient radiologic changes that occur between the post-surgical scan and post-radiation scan. Additionally, the mRANO criteria provides clear radiologic response rubrics for the assessment of pseudoprogression. Lesions that initially exhibit imaging characteristics suspicious for progressive disease are labeled as "preliminary progressive disease" and are later classified as either progressive disease or pseudoprogression based on imaging findings on subsequent evaluations. We use a more stringent 6-month follow-up time period to make these retrospective classifications because we believe this allows for more accurate classification. In prior similar studies some authors have used a 6-month follow-up time period [33], while others have used a 3-month time period [32, 35]. By using a more stringent 6-month time period we report a rate of pseudoprogression (22%) similar to the general rate reported in the literature (20–30%) [43–46]. In contrast, studies that used a 3-month time period reported a higher rate of pseudoprogression, ranging from 35 to 49% [32, 35].

A variety of ASL sequences exist and choice of ASL imaging technique and imaging parameters can heavily impact results. To promote standardization of data acquisition across scanner types, sites, and studies, a consensus white paper was previously released which provides recommendations for optimal ASL labeling approaches, readout approaches, and post-processing methods [25]. In accordance with the current consensus recommendations we chose a 3D PCASL sequence, which allows for higher

signal-to-noise ratio, SNR [23], less susceptibility artifact [25], and simpler clinical implementation [23]. Early studies that evaluated ASL for differentiation of treatment effects from recurrent glioma used a variety of less optimized ASL sequences which may have impacted results. For example, a prior study which used a single-slice pulsed ASL (PASL) method found that ASL images were qualitatively inferior to DSC-MR images [31]. Subsequent studies, including our own, which used 3D PCASL techniques have not supported this finding, indicating that this was likely technique related.

ASL offers several advantages over DSC-MRI. ASL is a non-contrast technique, therefore problems related to the use of GBCAs including NSF and neuronal tissue deposition are avoided [17, 18]. Additionally, because ASL is a non-contrast technique, problems related to contrast leakage at areas of blood–brain barrier breakdown are also avoided. This obviates the need for specifically tailored protocols accounting for the competing T1 and T2* effects seen with contrast leakage, meaning no need for preload bolus techniques, leakage correction algorithms, or flip angle corrections used in DSC-MRI [19–21]. Another important advantage of ASL is that it may provide improved lesion visualization and decreased susceptibility artifact compared to DSC-MRI. Newer implementations of ASL, like the 3D PCASL sequence, use fast-spin-echo techniques combined with spiral readout which provides decreased sensitivity to susceptibility artifacts compared to the gradient-echo techniques typically used in DSC-MRI. This is particularly valuable in GBM treatment response assessment because prominent susceptibility artifact is often present due to post-surgical changes, including residual blood products along the surgical margin, which can confound perfusion measurements. Prior qualitative studies have demonstrated that lesion visualization and susceptibility artifact is improved in 3D PCASL compared to DSC-MRI [26, 33, 34]. Our quantitative results support these findings. Detailed evaluation of the six cases where 3D PCASL correctly classified the lesion while DSC-MRI misclassified the lesion revealed that this often occurred at areas of prominent susceptibility artifact along the skull base, paranasal sinuses, and adjacent to large resection cavities with residual blood products, suggesting that ASL may outperform DSC-MRI in such cases.

Because ASL is a subtraction technique, a potential drawback of ASL compared to DSC-MRI is sensitivity to motion artifact. Qualitatively, the readers of this study did not encounter increased motion artifact in the ASL images compared to the DSC-MRI images. We suspect this may be because newer implementations of ASL incorporate background suppression which helps mitigate the effects of motion [25]. Furthermore, although 3D readouts are inherently more sensitive to motion, the 3D stack of spirals readout used allows for oversampling of the center of k-space and provides additional motion resistance.

A final potential advantage of ASL is that absolute, rather than relative, values of CBF can be easily measured. This is beneficial because absolute measurements may allow for cross-study comparisons and may facilitate longitudinal follow up. Absolute values can also be measured in DSC-MRI; however, this requires the additional calculation of the arterial input function and deconvolution [20], steps which are less easily and less routinely performed in current clinical applications of DSC-MRI. Two other studies have reported absolute ASL-CBF cut-off values for differentiation of progressive disease from pseudoprogression [32, 33], and in both studies the reported values are lower than what we report. We suspect this is because both prior studies were performed in mixed cohorts, which included patients with low-grade glioma, where perfusion measurements are expected to be lower. Although the use of a single absolute ASL-CBF cut-off value for differentiation of progressive disease from pseudoprogression is appealing, caution is advised because measurements are dependent on many factors including differences between scanners, ASL technique choice, and post-processing analysis method (mean ROI value, max ROI value, histogram analysis). These same cautions apply to DSC perfusion MRI techniques where measurements are relative rather than absolute, and quantitative values are dependent on additional factors including preload bolus techniques and post-processing leakage correction methods, making longitudinal comparisons and comparisons between studies difficult.

Several limitations to our study should be acknowledged. First, our study was conducted with a small sample size at a single institution. This approach was taken in order to focus on a more homogeneous sample of patients with GBM, however, the use of a small sample size can lead to overfitting and could conceivably inflate the performance we report. Second, although the mRANO framework was used to standardize the radiologic evaluation, there is inherent heterogeneity in the patient cohort including size and location of the tumor, extent of resection, and variable treatment plans following chemoradiation. Third, limited pathology was available for confirmation of diagnosis, especially for pseudoprogression. Fourth, no post-processing leakage correction was used in our implementation of DSC-MRI. To offset the expected increase in T1-weighting and resultant underestimation of rCBF and rCBV related to contrast leakage, we apply a preload bolus. Fifth, regarding the DSC-MRI protocol, a small subset of patients were scanned using an alternate contrast leakage correction schema. We acknowledge the mild heterogeneity in our DSC-MRI protocol, however, because there are numerous reported methods for contrast leakage correction in DSC-MRI without a single consensus standard and because the goal of our study was to evaluate qualitative differences between perfusion values (low or high) within subjects rather than to compare

quantitative values across studies, we do not believe this heterogeneity meaningfully impacts our results. Additionally, a subset analysis evaluating differences between the two DSC protocol groups demonstrated no significant difference. The protocol partially reflects current clinical implementations of DSC-MRI where heterogeneity in scanners, manufacturers, scanning parameters, and processing streams is not uncommon. Sixth, perfusion measurements were made using ROI-methods rather than more comprehensive histogram-analysis methods; however, this more accurately reflects current clinical practice where dedicated histogram analyses are less likely to be performed.

Conclusion

Our findings suggest that 3D PCASL and DSC perfusion MRI both differentiate progressive disease from pseudoprogression in patients with GBM with high accuracy. However, 3D PCASL is less sensitive to susceptibility artifact and may allow for improved classification in areas of prominent susceptibility artifact such as along the skull base and adjacent to large resection cavities with residual blood products.

Funding This study was supported by GE Healthcare GE14347180341 (N.F. and C.R.M.) and American Cancer Society RSG-15-229-01-CCE (C.R.M).

Compliance with ethical standards

Conflict of interest Carrie R. McDonald and Nikdokht Farid have received funding from GE Healthcare. David E. Piccioni is on the advisory board for Tocagen. Other authors report no conflicts of interest related to this study.

Ethical approval All procedures performed in studies involving human participants were in accordance with the ethical standards of the Institutional and/or National Research Committee and with the 1964 Helsinki Declaration and its later amendments or comparable ethical standards.

Informed consent Informed consent was obtained from all individual participants included in the study.

References

1. Ostrom QT, Gittleman H, Fulop J, Liu M, Blanda R, Kromer C, Wolinsky Y, Kruchko C, Barnholtz-Sloan JS (2015) CBTRUS Statistical Report: primary brain and central nervous system tumors diagnosed in the United States in 2008–2012. Neuro-oncology 17(Suppl 4):iv1–iv62
2. Stupp R, Hegi ME, Mason WP, van den Bent MJ, Taphoorn MJB, Janzer RC, Ludwin SK, Allgeier A, Fisher B, Belanger K, Hau P, Brandes AA, Gijtenbeek J, Marosi C, Vecht CJ, Mokhtari K, Wesseling P, Villa S, Eisenhauer E, Gorlia T, Weller M, Lacombe D, Cairncross JG, Mirimanoff R-O (2009) Effects of radiotherapy with concomitant and adjuvant temozolomide versus radiotherapy alone on survival in glioblastoma in a randomised phase III study: 5-year analysis of the EORTC-NCIC trial. Lancet Oncol 10(5):459–466
3. Stupp R, Mason WP, van den Bent MJ, Weller M, Fisher B, Taphoorn MJB, Belanger K, Brandes AA, Marosi C, Bogdahn U, Curschmann J, Janzer RC, Ludwin SK, Gorlia T, Allgeier A, Lacombe D, Cairncross JG, Eisenhauer E, Mirimanoff RO (2005) Radiotherapy plus concomitant and adjuvant temozolomide for glioblastoma. N Engl J Med 352(10):987–996
4. Wen PY, Macdonald DR, Reardon DA, Cloughesy TF, Sorensen AG, Galanis E, Degroot J, Wick W, Gilbert MR, Lassman AB, Tsien C, Mikkelsen T, Wong ET, Chamberlain MC, Stupp R, Lamborn KR, Vogelbaum MA, van den Bent MJ, Chang SM (2010) Updated response assessment criteria for high-grade gliomas: response assessment in Neuro-oncology Working Group. J Clin Oncol 28(11):1963–1972
5. Thust SC, van den Bent MJ, Smits M (2018) Pseudoprogression of brain tumors. J Magn Reson Imaging 48(3):571–589
6. Ellingson BM, Wen PY, Cloughesy TF (2017) Modified criteria for radiographic response assessment in glioblastoma clinical trials. Neurother J Am Soc Exp Neurother 14(2):307–320
7. Weller M, Cloughesy T, Perry JR, Wick W (2013) Standards of care for treatment of recurrent glioblastoma—are we there yet? Neuro-oncology 15(1):4–27
8. Rempp KA, Brix G, Wenz F, Becker CR, Guckel F, Lorenz WJ (1994) Quantification of regional cerebral blood flow and volume with dynamic susceptibility contrast-enhanced MR imaging. Radiology 193(3):637–641
9. Aronen HJ, Gazit IE, Louis DN, Buchbinder BR, Pardo FS, Weisskoff RM, Harsh GR, Cosgrove GR, Halpern EF, Hochberg FH et al (1994) Cerebral blood volume maps of gliomas: comparison with tumor grade and histologic findings. Radiology 191(1):41–51
10. Brem S (1976) The role of vascular proliferation in the growth of brain tumors. Clin Neurosurg 23:440–453
11. Plate KH, Mennel HD (1995) Vascular morphology and angiogenesis in glial tumors. Exp Toxicol Pathol 47(2–3):89–94
12. Wesseling P, van der Laak JA, de Leeuw H, Ruiter DJ, Burger PC (1994) Quantitative immunohistological analysis of the microvasculature in untreated human glioblastoma multiforme. Computer-assisted image analysis of whole-tumor sections. J Neurosurg 81(6):902–909
13. Hygino da Cruz LC, Rodriguez I, Domingues RC, Gasparetto EL, Sorensen AG (2011) Pseudoprogression and pseudoresponse: imaging challenges in the assessment of posttreatment glioma. Am J Neuroradiol 32(11):1978
14. Barajas RF Jr, Chang JS, Segal MR, Parsa AT, McDermott MW, Berger MS, Cha S (2009) Differentiation of recurrent glioblastoma multiforme from radiation necrosis after external beam radiation therapy with dynamic susceptibility-weighted contrast-enhanced perfusion MR imaging. Radiology 253(2):486–496
15. Hu LS, Baxter LC, Smith KA, Feuerstein BG, Karis JP, Eschbacher JM, Coons SW, Nakaji P, Yeh RF, Debbins J, Heiserman JE (2009) Relative cerebral blood volume values to differentiate high-grade glioma recurrence from posttreatment radiation effect: direct correlation between image-guided tissue histopathology and localized dynamic susceptibility-weighted contrast-enhanced perfusion MR imaging measurements. Am J Neuroradiol 30(3):552–558
16. Mangla R, Singh G, Ziegelitz D, Milano MT, Korones DN, Zhong J, Ekholm SE (2010) Changes in relative cerebral blood volume 1 month after radiation-temozolomide therapy can help predict overall survival in patients with glioblastoma. Radiology 256(2):575–584

17. Sadowski EA, Bennett LK, Chan MR, Wentland AL, Garrett AL, Garrett RW, Djamali A (2007) Nephrogenic systemic fibrosis: risk factors and incidence estimation. Radiology 243(1):148–157
18. McDonald RJ, McDonald JS, Kallmes DF, Jentoft ME, Murray DL, Thielen KR, Williamson EE, Eckel LJ (2015) Intracranial gadolinium deposition after contrast-enhanced MR imaging. Radiology 275(3):772–782
19. Boxerman JL, Schmainda KM, Weisskoff RM (2006) Relative cerebral blood volume maps corrected for contrast agent extravasation significantly correlate with glioma tumor grade, whereas uncorrected maps do not. Am J Neuroradiol 27(4):859–867
20. Welker K, Boxerman J, Kalnin A, Kaufmann T, Shiroishi M, Wintermark M (2015) ASFNR recommendations for clinical performance of MR dynamic susceptibility contrast perfusion imaging of the brain. Am J Neuroradiol 36(6):E41–E51
21. Paulson ES, Schmainda KM (2008) Comparison of dynamic susceptibility-weighted contrast-enhanced MR methods: recommendations for measuring relative cerebral blood volume in brain tumors. Radiology 249(2):601–613
22. Jackson A, O'Connor J, Thompson G, Mills S (2008) Magnetic resonance perfusion imaging in neuro-oncology. Cancer Imaging Off Publ Int Cancer Imaging Soc 8(1):186–199
23. Grade M, Hernandez Tamames JA, Pizzini FB, Achten E, Golay X, Smits M (2015) A neuroradiologist's guide to arterial spin labeling MRI in clinical practice. Neuroradiology 57(12):1181–1202
24. Wong EC (2014) An introduction to ASL labeling techniques. J Magn Reson Imaging 40(1):1–10
25. Alsop DC, Detre JA, Golay X, Günther M, Hendrikse J, Hernandez-Garcia L, Lu H, MacIntosh BJ, Parkes LM, Smits M, van Osch MJP, Wang DJJ, Wong EC, Zaharchuk G (2015) Recommended implementation of arterial spin-labeled perfusion MRI for clinical applications: a consensus of the ISMRM Perfusion Study Group and the European Consortium for ASL in dementia. Magn Reson Med 73(1):102–116
26. Järnum H, Steffensen EG, Knutsson L, Fründ E-T, Simonsen CW, Lundbye-Christensen S, Shankaranarayanan A, Alsop DC, Jensen FT, Larsson E-M (2010) Perfusion MRI of brain tumours: a comparative study of pseudo-continuous arterial spin labelling and dynamic susceptibility contrast imaging. Neuroradiology 52(4):307–317
27. Lehmann P, Monet P, de Marco G, Saliou G, Perrin M, Stoquart-Elsankari S, Bruniau A, Vallee JN (2010) A comparative study of perfusion measurement in brain tumours at 3 Tesla MR: arterial spin labeling versus dynamic susceptibility contrast-enhanced MRI. Eur Neurol 64(1):21–26
28. Warmuth C, Gunther M, Zimmer C (2003) Quantification of blood flow in brain tumors: comparison of arterial spin labeling and dynamic susceptibility-weighted contrast-enhanced MR imaging. Radiology 228(2):523–532
29. Noguchi T, Yoshiura T, Hiwatashi A, Togao O, Yamashita K, Nagao E, Shono T, Mizoguchi M, Nagata S, Sasaki T, Suzuki SO, Iwaki T, Kobayashi K, Mihara F, Honda H (2008) Perfusion imaging of brain tumors using arterial spin-labeling: correlation with histopathologic vascular density. Am J Neuroradiol 29(4):688–693
30. Cebeci H, Aydin O, Ozturk-Isik E, Gumus C, Inecikli F, Bekar A, Kocaeli H, Hakyemez B (2014) Assessment of perfusion in glial tumors with arterial spin labeling; comparison with dynamic susceptibility contrast method. Eur J Radiol 83(10):1914–1919
31. Ozsunar Y, Mullins ME, Kwong K, Hochberg FH, Ament C, Schaefer PW, Gonzalez RG, Lev MH (2010) Glioma recurrence versus radiation necrosis? A pilot comparison of arterial spin-labeled, dynamic susceptibility contrast enhanced MRI, and FDG-PET imaging. Acad Radiol 17(3):282–290
32. Wang Y-L, Chen S, Xiao H-F, Li Y, Wang Y, Liu G, Lou X, Ma L (2018) Differentiation between radiation-induced brain injury and glioma recurrence using 3D PCASL and dynamic susceptibility contrast-enhanced perfusion-weighted imaging. Radiother Oncol 129(1):68–74
33. Xu Q, Liu Q, Ge H, Ge X, Wu J, Qu J, Xu K (2017) Tumor recurrence versus treatment effects in glioma: a comparative study of three dimensional pseudo-continuous arterial spin labeling and dynamic susceptibility contrast imaging. Medicine 96(50):e9332–e9332
34. Ye J, Bhagat SK, Li H, Luo X, Wang B, Liu L, Yang G (2016) Differentiation between recurrent gliomas and radiation necrosis using arterial spin labeling perfusion imaging. Exp Ther Med 11(6):2432–2436
35. Jovanovic M, Radenkovic S, Stosic-Opincal T, Lavrnic S, Gavrilovic S, Lazovic-Popovic B, Soldatovic I, Maksimovic R (2017) Differentiation between progression and pseudoprogression by arterial spin labeling MRI in patients with glioblastoma multiforme. J BUON 22(4):1061–1067
36. Choi YJ, Kim HS, Jahng G-H, Kim SJ, Suh DC (2013) Pseudoprogression in patients with glioblastoma: added value of arterial spin labeling to dynamic susceptibility contrast perfusion MR imaging. Acta Radiol 54(4):448–454
37. Buckner JC, Shaw EG, Pugh SL, Chakravarti A, Gilbert MR, Barger GR, Coons S, Ricci P, Bullard D, Brown PD, Stelzer K, Brachman D, Suh JH, Schultz CJ, Bahary JP, Fisher BJ, Kim H, Murtha AD, Bell EH, Won M, Mehta MP, Curran WJ Jr (2016) Radiation plus procarbazine, CCNU, and vincristine in low-grade glioma. N Engl J Med 374(14):1344–1355
38. Larsen J, Wharton SB, McKevitt F, Romanowski C, Bridgewater C, Zaki H, Hoggard N (2017) '*Low grade glioma': an update for radiologists*. Br J Radiol 90(1070):20160600–20160600
39. Farid N, Almeida-Freitas DB, White NS, McDonald CR, Kuperman JM, Almutairi AA, Muller KA, VandenBerg SR, Kesari S, Dale AM (2014) Combining diffusion and perfusion differentiates tumor from bevacizumab-related imaging abnormality (BRIA). J Neurooncol 120(3):539–546
40. Perme M, Blas M, Turk S (2004) Comparison of logistic regression and linear discriminant analysis: a simulation study. Metod Zv 1:143–161
41. van West SE, de Bruin HG, van de Langerijt B, Swaak-Kragten AT, van den Bent MJ, Taal W (2016) Incidence of pseudoprogression in low-grade gliomas treated with radiotherapy. Neurooncology 19(5):719–725
42. Melguizo-Gavilanes I, Bruner JM, Guha-Thakurta N, Hess KR, Puduvalli VK (2015) Characterization of pseudoprogression in patients with glioblastoma: is histology the gold standard? J Neurooncol 123(1):141–150
43. Brandsma D, Stalpers L, Taal W, Sminia P, van den Bent MJ (2008) Clinical features, mechanisms, and management of pseudoprogression in malignant gliomas. Lancet Oncol 9(5):453–461
44. Chamberlain MC, Glantz MJ, Chalmers L, Van Horn A, Sloan AE (2007) Early necrosis following concurrent Temodar and radiotherapy in patients with glioblastoma. J Neurooncol 82(1):81–83
45. de Wit MCY, de Bruin HG, Eijkenboom W, Sillevis Smitt PAE, van den Bent MJ (2004) Immediate post-radiotherapy changes in malignant glioma can mimic tumor progression. Neurology 63(3):535–537
46. Taal W, Brandsma D, de Bruin HG, Bromberg JE, Swaak-Kragten AT, Sillevis Smitt PAE, van Es CA, van den Bent MJ (2008) Incidence of early pseudo-progression in a cohort of malignant glioma patients treated with chemoirradiation with temozolomide. Cancer 113(2):405–410